

Sparse 3D Point-cloud Map Upsampling and Noise Removal as a vSLAM Post-processing Step: Experimental Evaluation

Andrey Bokovoy^{1,2} and Konstantin Yakovlev^{2,3}

¹ Peoples Friendship University of Russia (RUDN University)
1042160097@rudn.university

² Federal Research Center "Computer Science and Control" of Russian Academy of Sciences

{bokovoy,yakovlev}@isa.ru

³ National Research University Higher School of Economics
kyakovlev@hse.ru

Abstract. The monocular vision-based simultaneous localization and mapping (vSLAM) is one of the most challenging problem in mobile robotics and computer vision. In this work we study the post-processing techniques applied to sparse 3D point-cloud maps, obtained by feature-based vSLAM algorithms. Map post-processing is split into 2 major steps: 1) noise and outlier removal and 2) upsampling. We evaluate different combinations of known algorithms for outlier removing and upsampling on datasets of real indoor and outdoor environments and identify the most promising combination. We further use it to convert a point-cloud map, obtained by the real UAV performing indoor flight to 3D voxel grid (octo-map) potentially suitable for path planning.

Keywords: 3D · point-cloud · outlier removal · upsampling · vSLAM · 3D path planning · sparse map · feature-based vSLAM

1 Introduction

Simultaneous localization and mapping (SLAM) is a well-known problem in mobile robotics, which is considered for a variety of different applications [1,2] and platforms [3,4], with unmanned aerial or ground vehicles being the most widespread robots to use SLAM as part of the navigation loop [5,6,7]. There exists no universal SLAM method suitable for all robotic platforms and applications due to limitations these platforms/applications impose. Among the factors that influence SLAM the most one can name the following: available data (which in turn depends on the sensors type) and available computing capacities. One of the most challenging scenarios for SLAM is when only video-data, obtained from a single camera, is available and computational resources are limited. This is a typical scenario for UAV navigation, and it leads to so-called monocular vision-based SLAM (vSLAM) [8]. vSLAM methods rely on the single-camera video-flow

to construct (preferably in real-time) consistent 3D map of the unknown environment and can be classified into 2 major groups: indirect (or feature-based) and direct (dense and semi-dense) methods.

Indirect vSLAM algorithms utilize images' features [9] for mapping purposes. Thus the obtained map consists of the set of reconstructed image-features appropriately placed in 3D space. Since the amount of such features for every image is limited and is far less than image's size, the reconstructed map is likely to be sparse and contain large amount of free space (which is actually not free w.r.t obstacles) between the features. On the other hand, most of the feature-detectors utilized in vSLAM work fast (achieving real-time performance) and are invariant to image distortions, light, scale, rotation, etc., which makes them well-suited for real-world robotics applications.

Direct methods, like LSD-SLAM [10,11] or D-TAM [12] use the entire images to reconstruct the map, leading to dense (or semi-dense) maps with large amount of environment details captured. These methods are sensitive to the input data, e.g. they can not handle well distortions, rolling shutter and other typical noise disturbances. They can not run in real-time (without GPU acceleration) as well. One should also mention direct vSLAM methods based on machine learning techniques (e.g. convolutional neural networks), see [13,14] for example, that have appeared recently. Unfortunately, they require significant computational resources and time to learn before application.

Obviously an ideal vSLAM method should combine the strengths of both approaches, e.g. it should construct detailed maps like direct algorithms do and be fast and robust like indirect ones are. In order to achieve such performance, we suggest to post-process sparse maps, produced by feature-based vSLAM algorithms in order to make them more detailed and suitable for solving further navigation tasks (like path planning [15,16,17], control [18] etc.). Such an approach potentially leads to producing detailed maps of the environment with no extra computing costs associated with running direct vSLAM methods.

In this work we study different post-processing techniques, e.g. outlier removal and upsampling, applied to 3D sparse point-cloud maps generated by state-of-the-art feature-based vSLAM algorithms. We evaluate different techniques on various datasets (indoor and outdoor) to find the best combination. We further use it to construct the octo-map of the indoor environment which was not the part of the training datasets.

2 Problem Statement

2.1 vSLAM problem definition

The vision-based simultaneous localization and mapping problem for monocular camera (monocular vSLAM) is defined as follows. Let the matrix $I_t \in \mathbb{R}^{m \times n}$ denote the image of $m \times n$ pixels, obtained by the robot at time step t^1 . Thus the video-flow \mathbf{I}_T is the sequence $\mathbf{I}_T = \{I_t \mid t \in [1, T]\}$, where T is the end-time.

¹ For the sake of simplicity we assume that the image is grayscale and pixels are real numbers.

Given \mathbf{I}_T , the localization task is to compute positions of the camera in the global coordinate frame: $\mathbf{X}_T = \{\mathbf{x}_t \mid \mathbf{x}_t = (x, y, z, \alpha, \beta, \gamma)\}$, where x, y, z are translation coordinates and α, β, γ are the orientation angles (e.g. pitch, roll and yaw).

Furthermore, for each I_t we need to find a set of image points $P_t = \{p_i \mid i \leq K \leq m \times n\}$, $P_t \in 2^{I_t}$, such that $P_t = f_{proj}(E, t)$, where $E = \{e_l \mid e_l \in \mathbb{R}^3\}$ is the environment and f_{proj} is the function, that projects 3D points from current observation (E, t) to the 2D image I_t as P_t .

Finally, the map \mathbf{M} should be constructed using all the observations:

$$\begin{aligned} M_t &= \{f_{proj}^{-1}(p_i) \mid i \leq m \times n, p_i \in P_t\} \\ \mathbf{M} &= \bigcup_{t=1}^T M_t, \\ \mathbf{M} &= \{m_i \mid m_i \in \mathbb{R}^3\}. \end{aligned} \tag{1}$$

2.2 Map post-processing problem definition

Consider a filter that is function $filt : \mathbb{R}^3 \rightarrow 2^{\mathbb{R}^3}$ and a post-processed map, $\widehat{\mathbf{M}}$, that is constructed by sequentially applying the limited number of filters to the initial map: $\widehat{\mathbf{M}} = filt_1 \circ filt_2 \circ \dots \circ filt_H(\mathbf{M})$.

We now want to find such combination of filters that enriches the map with additional points (the map becomes more dense) and at the same time keeps the model as close to the ground-truth as possible. Formally, $|\widehat{\mathbf{M}}|$ should be maximized and $Error(\widehat{\mathbf{M}}, E)$ should be minimized, where $Error(\widehat{\mathbf{M}}, E) = \frac{1}{|\widehat{\mathbf{M}}|} \sum_{r=1}^{|\widehat{\mathbf{M}}|} \|\widehat{m}_r - e_r\|$, $m_r \in \widehat{\mathbf{M}}$, $e_r = corr(m_r)$ – correspondence function between E and $\widehat{\mathbf{M}}$ (Euclidean distance, for example).

3 Evaluated Methods and Algorithms

We need to choose a suitable vSLAM method, which is able to produce maps that can be further used (possibly after the described post-processing phase) for various navigation tasks, with path planning being of the main interest. This method should be applicable to real-world robotic applications, e.g. it should be i) fast (able to process at least 640×480 grayscale images at 30 Hz), ii) able to work with distorted images, iii) well studied and its implementation should be available for the community. Based on these criteria and taking into account the considerations specified in section 1, ORB-SLAM2 [19] was chosen. We also took into account the evaluation results of [20].

The results of running ORB-SLAM2 on real data collected by the compact quadcopter, performing its flight in the indoor environment of our institute, are shown on Fig. 1.

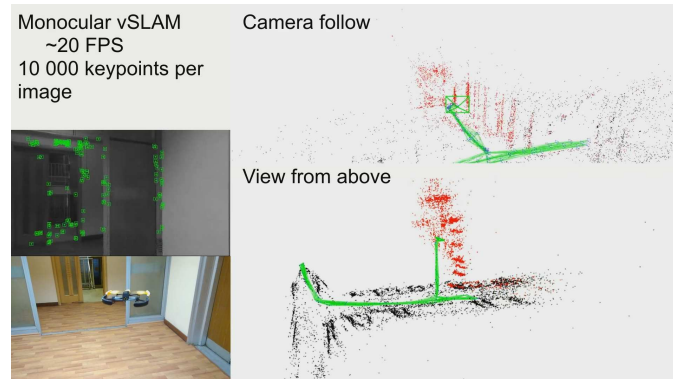


Fig. 1. ORB-SLAM2 output on real-world indoor flight performed by Parrot Bebop quadrotor. Video is available at <https://www.youtube.com/watch?v=piuVq8f61gs>

As one can see on Fig.1, ORB-SLAM2 map is sparse and noisy. To make the output more suitable for further conversion to the octomap (3D grid) [21] we suggest applying 2 following steps: i) outlier removal, ii) upsampling.

3.1 Outlier removal

There exists 2 general approaches to outlier removal for point-clouds: radius-based and statistical [22]. Radius-based methods filters the elements of the point-cloud based on the amount of neighbors they have. It iterates over input point-cloud once and retrieves the number of neighbors within the certain radius r . If this number is less than the predefined threshold b the point is considered an outlier.

Statistical approaches iterate through the input point-cloud twice. During the first iteration average distance from each point to its nearest l neighbors is estimated. Consequently, the mean and standard deviation are computed for all the distances in order to determine a threshold. On the second iteration the points will be considered as outliers if their average neighbor distance is above this threshold. The main parameter of statistical methods is the standard deviation multiplier h that affects the final threshold.

3.2 Upsampling

Almost all upsampling filters for point-clouds are based on Moving Least Squares (MLS) [23] techniques. This techniques involve the projecting of the point-clouds into continuous surface that minimizes a local least-square error. We choose the most common upsampling methods, such as Sample Local Plane, Random Uniform Density and Voxel Grid Dilation [24] for further evaluation. These methods are parameter-dependent and the parameters are: i) upsampling radius (u_r), upsampling step size (u_{sz}) and maximum number of upsampling steps (u_s) for

Sample Local Plane, ii) point density (d) for Random Uniform Density, iii) dilation voxel size (s_{vs}) and dilation iterations (d_i) for Voxel Grid Dilation.

3.3 Map scaling

For upsampling and outlier removal methods we need to find the best parameters at which this algorithms produce the most accurate and detailed maps. For this purposes, we need to compare the output of each method and their combinations with ground truth. Since ORB-SLAM2 produces the maps with unknown scaling, we need find corresponding points (algorithm 1) and adjust the scaling of ORB-SLAM2's map and ground truth (algorithm 2).

Algorithm 1 Corresponding points search.

1. Get $\mathbf{M}, \mathbf{X}_T, P_T = \{P_i\}, i \in [1, T]$ for ground-truth and $\widehat{\mathbf{M}}, \mathbf{X}'_T$ for post-processed map.
 2. Get \mathbf{I}_T with corresponding ground-truth E_T
 3. **for** each $I_i \in \mathbf{I}_T$
 4. **for** each pix $pix \in I_i$
 5. **if** $pix \in f_{proj}(E_i)$
 6. find the correspondence p' for pix in $\widehat{\mathbf{M}}$ if exists
 7. add p' to P'_i
 8. **end if**
 9. **end for**
 10. **for** each $m_i \in \mathbf{M}$ with $m'_i \in \widehat{\mathbf{M}}$ with correspondences P'_i
 11. Calculate per coordinate deviation: $D_i = m_i - \widehat{m}'_i$
 12. Add D_i to D
 13. **end for**
 14. **end for**
 15. **return** D
-

Algorithm 2 Map scaling.

1. Get an the resultant map $\widehat{\mathbf{M}}$ with corresponding trajectory \mathbf{X}'_T
 2. For ground truth map \mathbf{M} and trajectory \mathbf{X}_T adjust the x_1 pose to x'_1, x_T to x'_T and x_l with x'_l , where $l \in (1, T), l \in N$
 3. Find the scale factor $s = (s_x, s_y, s_z)$ for each coordinate x, y, z using translation of the poses \mathbf{X}'_T
 4. **return** $\widehat{\mathbf{M}} = \{s \circ m'_{pp_i}, i \in [1, K]\}$
-

4 Experimental Analysis and Results

Experimental evaluation consists of 2 main stages: **parameters adjustment** and **map quality estimation**. During the first stage we used limited amount of input data to adjust the parameters of outlier removal and upsampling filters. We also searched for best combination of the upsampler and the outlier removal. On the second step, we extrapolated the estimated parameters to a large variety of input data to estimate the quality of post-processed map. After all, we evaluated the suggested pipeline on the real-world scenario depicted in Fig.1.

4.1 Tools

We used open-source realization of ORB-SLAM2 ², provided by its authors for sparse map construction and PointCloud Library (PCL) [25] with built-in implementations of upsampling and outlier removal algorithms for map enhancement. Experiments were run on the 3-PC cluster with each experiment executed in it's own processor's thread.

2 datasets were used: TUMindoor Dataset [26] and Malaga Dataset 2009 [27]. Malaga Dataset 2009 consists of 6 outdoor environments with ground-truth map, 6-DOF camera poses and corresponding video sequences. TUMindoor Dataset consists of the sequences, gathered inside of Technische Universitt Mnchen with ground-truth map and 6-DOF camera poses. The path length varies from 120m to 1169m. We split each initial sequence form the datasets into smaller sequences with a fixed path length of 10m, thus 45 sequences from Malaga Dataset and 65 sequences from TUMindoor Dataset were used. The example of the provided environment is shown in Fig.2.

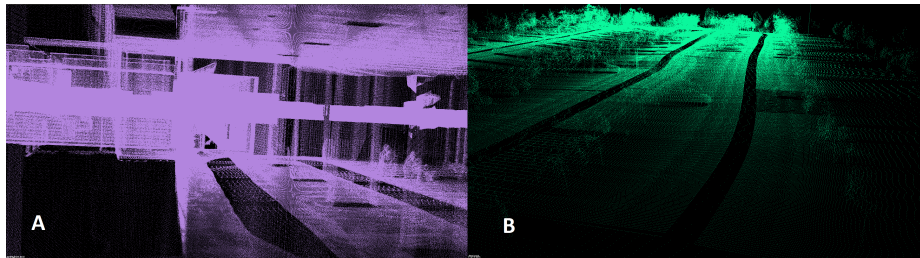


Fig. 2. Datasets, used for experimental evaluation. (a) TUMindoor Dataset (b) Malaga Dataset 2009

4.2 Parameters adjustment

To adjust the parameters we used TUM RGBD-SLAM Dataset and Benchmark [28], particularly the “freiburg2_desk_validation” sequence.

² https://github.com/raulmur/ORB_SLAM2

We varied each parameter described in section 3 for each of the upsampling and outlier removal method. 25 000 of the parameters' combinations were evaluated in total. We estimated the runtime, resultant map size and map's accuracy compared to ground-truth. The results for best parameterizations are shown in Table 1. As one can see, the best performance is achieved by statistical outlier with $h = 1.8$ and by Voxel Grid Dilation with dilation voxel size set to 4.9 and dilation iterations set to 3.

Table 1. Map accuracy and processing time.

Algorithm	Parameters	Deviation in % (compared to ground-truth)	Time (s)	Map points
ORB-SLAM2	-	2.81	-	11 546
Radius filter	$b = 4$ $r = 8.9$	2.34	4	85 982
Statistical filter	$h = 1.8$	2.01	1.52	87 449
Sample Local Plane	$u_r = 1.12$ $u_s z = 0.58$ $u_s = 118$	1.98	3.2	90 178
Random Uniform Density	$d = 13$	2.13	4	89 965
Voxel Grid Dilation	$s_{vs} = 4.9$ $d_i = 3$	1.83	2.1	95 676

4.3 Map Quality Estimation

We combined the statistical outlier filter with Voxel Grid Dilation upsampling algorithm to post-process the maps obtained by ORB-SLAM2 on all the available data: 110 data instances from both TUMidoor Dataset and Malaga Dataset. The results of the evaluation are shown in Fig.3. As one can see, the suggested approach is able to produce more precise and dense maps, compared to original ORB-SLAM2.

Finally we tested the suggested pipeline on the video-data, captured from Bebop quadrotor performing indoor flight in our lab (video is available at <https://www.youtube.com/watch?v=piuVq8f61gs>) The visualization of the result is given on Fig. 4. Original map contains 8838 points, smoothed map has 6832 and upsampled map - 58416. As one can see, applying the suggested outlier removal and upsampling filters positively influence the quality of the resultant point-cloud map and, as a result, converted octo-map becomes more suitable for further usage (e.g. for path planning).

5 Conclusion

We have considered the problem of enhancing the maps produced by monocular feature-based vSLAM (ORB-SLAM2). This problem naturally arises in various

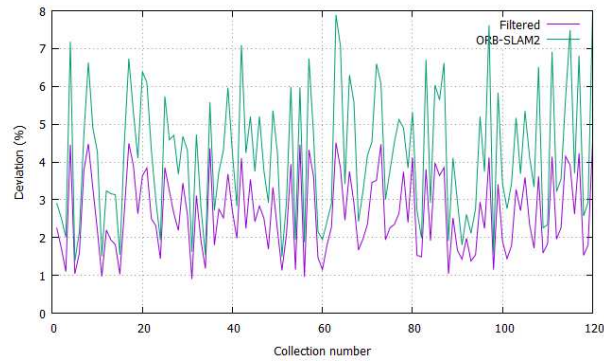


Fig. 3. Average deviation of the post-processed map and ORB-SLAM2's map from ground-truth. Less is better.

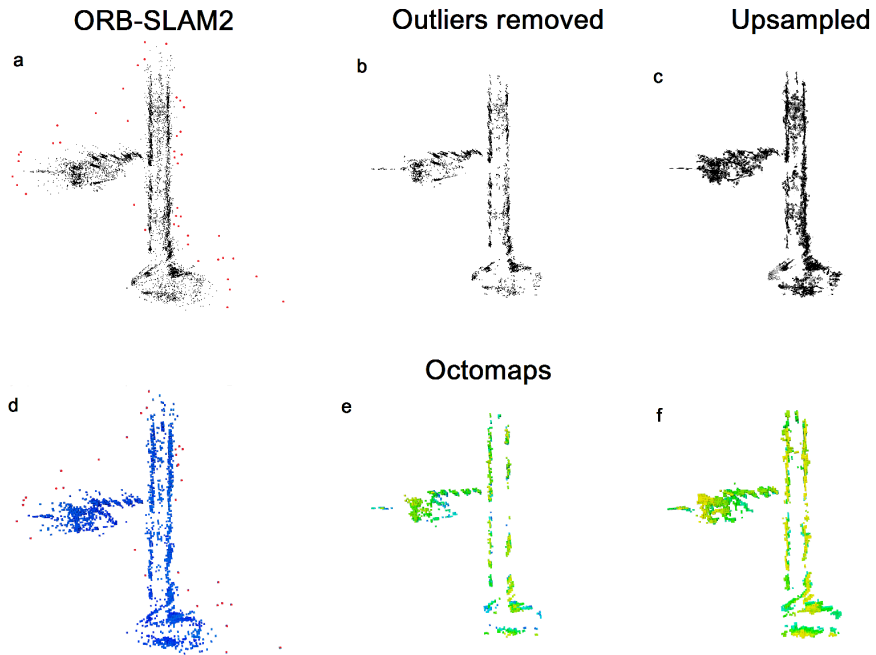


Fig. 4. a) Original map, produced by ORB-SLAM2 (outliers are highlighted in red); b) the map with outliers removed; c) upsampled map. d), e), f) – corresponding octrees (with the ceiling and the floor removed for better visualization).

mobile robotics applications as typically the feature-based vSLAM maps are extremely sparse. We evaluated the post-processing pipeline that includes outlier removal and upsampling. Different combinations of known methods were evaluated and the best parameters for each method were identified. The best combination was then extensively tested on both well-known in the community indoor and outdoor collections of video-data and the video from real quadrotor captured in our lab. The results of such evaluation showed the increase of the accuracy and the density of the post-processed maps.

Acknowledgment This work was partially supported by the “RUDN University Program 5-100” and by the RFBR project No. 17-29-07053.

References

1. Cadena, C., Carlone, L., Carrillo, H., Latif, Y., Scaramuzza, D., Neira, J., Reid, I., Leonard, J.: Past, present, and future of simultaneous localization and mapping: Towards the robust-perception age. *IEEE Transactions on Robotics* **32**(6) (2016) 13091332
2. Balan, A., Flaks, J., Hodges, S., Isard, M., Williams, O., Barham, P., Izadi, S., Hiliges, O., Molyneaux, D., Kim, D., et al.: Distributed asynchronous localization and mapping for augmented reality (January 13 2015) US Patent 8,933,931.
3. Li, R., Liu, J., Zhang, L., Hang, Y.: LIDAR/MEMS IMU integrated navigation (SLAM) method for a small UAV in indoor environments. In: *Inertial Sensors and Systems Symposium (ISS), 2014 DGON, IEEE* (2014) 1–15
4. Leonard, J.J., Bahr, A.: Autonomous underwater vehicle navigation. In: *Springer Handbook of Ocean Engineering*. Springer (2016) 341–358
5. Caballero, F., Merino, L., Ferruz, J., Ollero, A.: Vision-based odometry and SLAM for medium and high altitude flying UAVs. *Journal of Intelligent and Robotic Systems* **54**(1-3) (2009) 137–161
6. Sazdovski, V., Silson, P.M.: Inertial navigation aided by vision-based simultaneous localization and mapping. *IEEE Sensors Journal* **11**(8) (2011) 1646–1656
7. Vu, Q., Nguyen, V., Solenaya, O., Ronzhin, A., Mehmet, H.: Algorithms for joint operation of service robotic platform and set of UAVs in agriculture tasks. In: *Advances in Information, Electronic and Electrical Engineering (AIEEE), 2017 5th IEEE Workshop on, IEEE* (2017) 1–6
8. Buyval, A., Afanasyev, I., Magid, E.: Comparative analysis of ROS-based monocular SLAM methods for indoor navigation. In: *Proceedings of the Ninth International Conference on Machine Vision (ICMV 2016)*. (2017) 10341–10341
9. Rublee, E., Rabaud, V., Konolige, K., Bradski, G.: ORB: An efficient alternative to SIFT or SURF. In: *Computer Vision (ICCV), 2011 IEEE international conference on, IEEE* (2011) 2564–2571
10. Engel, J., Schöps, T., Cremers, D.: LSD-SLAM: Large-scale direct monocular SLAM. In: *European Conference on Computer Vision, Springer* (2014) 834–849
11. Bokovoy, A., Yakovlev, K.: Enhancing semi-dense monocular vSLAM used for multi-rotor UAV navigation in indoor environment by fusing IMU data. In: *The 2018 International Conference on Artificial Life and Robotics (ICAROB2018), ALife Robotics Corporation Ltd.* (2018) 391–394

12. Newcombe, R.A., Lovegrove, S.J., Davison, A.J.: DTAM: Dense tracking and mapping in real-time. In: *Computer Vision (ICCV), 2011 IEEE International Conference on*, IEEE (2011) 2320–2327
13. Tateno, K., Tombari, F., Laina, I., Navab, N.: CNN-SLAM: Real-time dense monocular SLAM with learned depth prediction. *arXiv preprint arXiv:1704.03489* (2017)
14. Makarov, I., Aliev, V., Gerasimova, O.: Semi-dense depth interpolation using deep convolutional neural networks. In: *Proceedings of the 2017 ACM on Multimedia Conference. MM '17*, New York, NY, USA, ACM (2017) 1407–1415
15. Yakovlev, K., Baskin, E., Hramoin, I.: Grid-based angle-constrained path planning. In Hölldobler, S., Peñaloza, R., Rudolph, S., eds.: *KI 2015: Advances in Artificial Intelligence*, Cham, Springer International Publishing (2015) 208–221
16. Magid, E., Tsubouchi, T., Koyanagi, E., Yoshida, T.: Building a search tree for a pilot system of a rescue search robot in a discretized random step environment. *Journal of Robotics and Mechatronics* **23**(4) (2011) 567
17. Makarov, I., Polyakov, P.: Smoothing voronoi-based path with minimized length and visibility using composite bezier curves. In: *AIST (Supplement)*. (2016) 191–202
18. Buyval, A., Gabdulin, A., Mustafin, R., Shimchik, I.: Deriving overtaking strategy from nonlinear model predictive control for a race car. In: *2017 IEEE/RSJ International Conference on Intelligent Robots and Systems (IROS 2017)*. (Sept 2017) 2623–2628
19. Mur-Artal, R., Tardós, J.D.: ORB-SLAM2: An Open-Source SLAM System for Monocular, Stereo, and RGB-D Cameras. *IEEE Transactions on Robotics* (2017)
20. : Kitti vision benchmark suite. http://www.cvlibs.net/datasets/kitti/eval_odometry.php Accessed: 2018-06-22.
21. Hornung, A., Wurm, K.M., Bennewitz, M., Stachniss, C., Burgard, W.: OctoMap: An efficient probabilistic 3d mapping framework based on octrees. *Autonomous Robots* **34**(3) (2013) 189–206
22. Rusu, R.B., Marton, Z.C., Blodow, N., Dolha, M., Beetz, M.: Towards 3D point cloud based object maps for household environments. *Robotics and Autonomous Systems* **56**(11) (2008) 927–941
23. Reuter, P., Joyot, P., Trunzler, J., Boubekeur, T., Schlick, C.: Surface reconstruction with enriched reproducing kernel particle approximation. In: *Point-Based Graphics, 2005. Eurographics/IEEE VGTC Symposium Proceedings*, IEEE (2005) 79–87
24. Skinner, B., Vidal Calleja, T., Valls Miro, J., De Bruijn, F., Falque, R.: 3D point cloud upsampling for accurate reconstruction of dense 2.5 D thickness maps. In: *Australasian Conference on Robotics and Automation*. (2014)
25. Rusu, R.B., Cousins, S.: 3d is here: Point cloud library (pcl). In: *Robotics and automation (ICRA), 2011 IEEE International Conference on*, IEEE (2011) 1–4
26. Huitl, R., Schroth, G., Hilsenbeck, S., Schweiger, F., Steinbach, E.: TUMindoor: An extensive image and point cloud dataset for visual indoor localization and mapping. In: *Image Processing (ICIP), 2012 19th IEEE International Conference on*, IEEE (2012) 1773–1776
27. Blanco, J.L., Moreno, F.A., Gonzalez, J.: A collection of outdoor robotic datasets with centimeter-accuracy ground truth. *Autonomous Robots* **27**(4) (2009) 327
28. Sturm, J., Engelhard, N., Endres, F., Burgard, W., Cremers, D.: A benchmark for the evaluation of RGB-D SLAM systems. In: *Intelligent Robots and Systems (IROS), 2012 IEEE/RSJ International Conference on*, IEEE (2012) 573–580